JOURNAL OF MATERIALS SCIENCE 25 (1990) 3359–3367

The relation of hardness to toughness and retained austenite content in N_2–H_2–CH_4 sintered T6, T15 and T42 high-speed steels

V. MARTÍNEZ*, R. PALMA*, J. J. URCOLA‡
*Escuela Superior de Ingenieros Industriales de San Sebastián, Urdaneta 9, 20009 San Sebastián, Spain
‡Centro de Estudios e Investigaciones Técnicas de Guipúzcoa (CEIT), Pº de Manuel de Lardizabal, 15, Barrio de Ibaeta, 20009 San Sebastián, Spain

The increase of toughness, 10 to 35 MPa $m^{1/2}$, with decreasing hardness, V_H 950 to 500, is reported for sintered T6, T15 and T42 high-speed steels. This range of properties resulted from combinations of sintering temperatures (in N_2–H_2–CH_4), HIPping and tempering treatments of steels processed from water-atomized powders. Toughness is related to the properties of the matrix, but more specifically to the retained austenite content, varying between 5% (HV10 $\simeq$ 950, $K_{IC} \simeq 10$ MPa $m^{1/2}$) and 70% (HV10 $\simeq$ 500, $K_{IC} \simeq 35$ MPa $m^{1/2}$). Austenite retention is caused by the stabilizing affect of nitrogen (0.3 to 0.7%), picked up from the sintering atmosphere. Fractographic examination revealed that, although failure proceeded by complex modes that could be described mainly as quasi-cleavage, microplasticity was observed in the high austenite materials, as opposed to the flatter fracture surfaces, with much less plasticity apparent, for the lower retained austenite-containing materials.

1. Introduction

High-speed steels have been traditionally used as cutting tools and continue to be so. Increasingly, however they are employed in wear and fatigue resistant applications. For bearings and other wear-resistant components, high hardness in the surface together with toughness in the core are normally required. This is, for instance, the case in mainshaft bearings for aerogas turbine engines, for which high-speed steel (HSS), T1 as well as M50 is currently employed [1]. The increasing sizes and rotational speeds require an optimum combination between the core toughness, to resist the potential catastrophic propagation of transverse cracks, and the surface hardness, to cope with the big loads of rolling contact fatigue. Minimum fracture toughness values of 35 MN $m^{-3/2}$ are now proposed, approximately double the currently attainable K_{Ic} of both T1 and M50 [2, 3]. Although the US approach to reaching these values seems directed towards the use of surface hardened bearings, especially M50 NiL, the increasing service temperatures of the newly required bearings, perhaps reaching in some cases 350° C, makes appropriate consideration of continued use of high-speed steels in this application [2, 3].

Averbach *et al.* [1] reported K_{Ic} values of 50 MN $m^{-3/2}$ in M50NiL, a modified M50 steel with a 3.5% nickel and a low carbon content of 0.1%. This is a significant improvement in fracture toughness, when compared with 18 MN $m^{-3/2}$ found in conventional M50 [4]. Whereas the preference in the USA for mainshaft bearings is M50, grade BT1 is generally used in the UK. Rescalvo and Averbach [3] also studied the fracture toughness of BT1 and found values of 18 MN $m^{-3/2}$, similar to those for M50, in spite of the large microstructural differences. These authors postulate, along with others [5, 6], that the fracture toughness depends mainly on the matrix microstructure and properties, with the amount, the size and the morphology of carbides having only a marginal affect.

Other authors [7–9] argue that, although the total amount of carbides does not play an important role in determining the value of K_{Ic}, the distribution, morphology and size of primary carbides have an important influence on the fracture process in these steels. Wronski *et al.* [10] and Shelton and Wronski [11] have reported that, in high-speed steels with a low inclusion content and without porosity, fracture initiation usually occurs in carbide clusters. Powder metallurgy offers a good way of producing high-speed steels without these clusters, either by sintering directly to full density, or by undersintering to closed porosity and subsequent hot isostatic pressing, HIPping, to eliminate the porosity, or by the HIP route employing gas atomized powders.

Important improvements in fracture toughness using powder metallurgy processing are already reported in the literature. In particular at room temperature values up to 30 MN $m^{-3/2}$ for T1 and T6 and up to 48 MN $m^{-3/2}$ in the temperature range 200 to 400° C for T6 [11] have been reported.

In the present work the fracture toughness – after several heat treatments – of three high speed steels

0022–2461/90 $03.00 + .12

grades: T15, T42 and T6, obtained by sintering in an industrial atmosphere (90% N_2, 9% H_2 and 1% CH_4) has been measured. Also some T15 and T6 specimens have been HIPped, for T15 fracture toughness values were compared with those obtained after direct sintering. In this sintering process, due to the presence of a high amount of nitrogen in the atmosphere, an important nitrogenation of the steel takes place. As reported previously [12] 0.4 to 0.5% weight gains of nitrogen are obtained. This element stabilizes the austenite, thus tempering treatments different to those used for the same steels when vacuum sintered have to be employed to eliminate the retained austenite. In this work its amount was controlled and thus for these steels the influence of retained austenite on fracture toughness has been investigated.

2. Experimental procedure

The chemical compositions of the water atomized high speed steel powders used in the present investigation are given in Table I. The T15 and T42 powders were bought from Powdrex Ltd and the T6 (supplied by the Mechanical Engineering Department of the University of Bradford) was atomized by Davy McKee.

The powders were mixed for 2 h with an addition of 0.2% high purity graphite. Specimens of 30 g nominal weight were uniaxially pressed in a 16 mm diameter die using a pressure of 500 MN m^{-2}, to obtain greens of approximately 64% TD (Full theoretical density). Sintering was carried out in an independently controlled three-zone Lindberg furnace provided with a refractory steel chamber. A 90% N_2, 9% H_2 and 1% CH_4 atmosphere was used for sintering.

The optimal sintering conditions for each steel: gas flow, temperature and time, have been described elsewhere [13]. After sintering for 1 h at 1240° C and 1316° C for T15 and T6 steels, respectively and 45 min at 1215° C for T42 steel, densities equal to or higher than 99% TD were obtained. Also some samples of T15 steel were undersintered, for 1 h at 1215° C, and subsequently HIPped. The different combinations of temperatures and pressures for a cycle of 45 min of HIPping for T15 and T6 steels are given in Table II.

Annealing for 1 h at 900° C and cooling, at a mean rate of 20° C h^{-1} down to 680° C and subsequently at 100° C h^{-1} to room temperature, was necessary to reduce the hardness of T42 to 340 HV10 and that of T15 to 360 HV10. In the T6 case it was not necessary to anneal due to the low hardness (410 HV10) of the as-sintered specimens. Before austenitizing and quenching, the annealed cylinders, 12.0 mm in diameter and of 18.0 mm height, were machined to 'short rod' (Barker) specimens for fracture toughness testing, according to the dimensions given in Fig. 1.

TABLE I Chemical composition (wt %) of the as-received high-speed steel powders

	C	Cr	Co	Mo	V	W	Ni	Mn	Si	O_2(p.p.m)
T15	1.64	4.37	4.99	0.56	4.70	12.40	0.13	0.24	0.25	794
T42	1.43	4.18	9.44	3.22	2.94	8.82	–	0.21	0.28	530
T6	0.75	4.35	12.5	0.40	1.51	20.24	–	–	–	1830

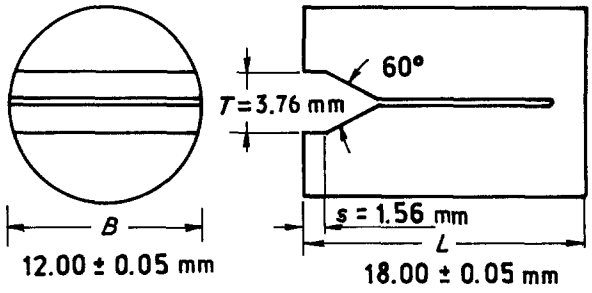

Figure 1 Short rod test specimen geometry for fracture toughness testing.

After machining the specimens were austenitized in a muffle furnace, using the sintering atmosphere to avoid decarburization, for 3 min at the temperatures given in Table III, and quenched in oil. Final heat treatments consisted of triple tempering of 1 h each at the temperatures also indicated in Table III; several tempering temperatures were used for each material. The mean linear intersection technique was used to measure the grain size of specimens quenched from different austenitizing temperatures; a minimum of 500 intersections were counted.

Short rod (Fractometer) fracture toughness tests were performed in a screw driven universal Instron machine at a speed of mouth opening of 0.5 mm min^{-1}. This kind of test, as reported by Barker [14], does not need previous precracking, because the specimen geometry is such that a crack is created and progresses in a stable way, up to a certain critical length (a_c), when the maximum load is reached L_{max}; thence it grows in an unstable way. From the maximum load and the specimen geometrical factors, the fracture toughness is calculated as

$$K_Q = \frac{AL_{max}}{B^{3/2}} \quad (1)$$

where A is a factor depending on the geometry, and takes a value of $A = 22$ [14], and B is the specimen diameter. K_Q is the fracture toughness in the linear elastic mechanics approximation (which holds well for notched T6, T15 and T42 steels). Nevertheless, slight non-linearity in the load–deflection curves was sometimes observed (as also reported for cemented carbides and other high speed steels [15]. This has been interpreted as caused by internal stresses rather than plasticity.

The correction for both effects is done through a factor called p. The value of p is determined by loading and unloading cycles during the test [16]. The fracture toughness after the p correction becomes

$$K_{Ic} = K_Q \left(\frac{1+p}{1-p}\right)^{1/2} \quad (2)$$

TABLE II Parameters used for the HIPping operation

Material	Temperature (° C)	Pressure (MPa)	Time (min)
T15–H1	1190	160	45
T15 H2	1210	140	45
T6	1290	140	45

The radius of the plastic zone, r_p, at the crack tip, was estimated using the expression

$$r_p = \frac{1}{6\pi}\left(\frac{K_{IC}}{\sigma_y}\right)^2 \quad (3)$$

where σ_y was obtained using the approximation $\sigma_y \simeq (HV10)/3$.

Fractographic examination was performed on one of the fracture faces of the short rod specimens in a Philips 501B scanning electron microscope. The other face, after polishing, was used for metallographic observations, hardness measurement and for the determination of retained austenite. This was measured using X-ray diffraction techniques, using the method proposed by Miller [17]

$$\%\ \gamma_{ret} = \frac{1.4I_\gamma}{I_\alpha + 1.4I_\gamma} \quad (4)$$

where

$$I_\gamma = \frac{I_{\gamma 220} + I_{\gamma 311}}{2}\ y\ I_\alpha = I_{\alpha 211} \quad (5)$$

The distribution of particles and their chemical compositions were analysed also in these polished unetched surfaces using 501B SEM fitted with an EDAX 9100 microanalytical system.

3. Results

The austenitic grain size was 14.1 ± 0.9 μm for T42 steel when austenitized at 1160° C and 15.4 ± 0.9 μm when austenitized at 1190° C. For steel T15, after austenitizing at 1210° C, it was 21.1 ± 0.9 μm for the directly sintered material, 20.2 ± 0.7 μm for T15 H1 and 20.4 ± 0.9 μm for T15 H2. Steel T6 had a 14.7 ± 0.5 μm grain size after austenitizing at 1275° C.

In all three steels metallographic observation revealed the presence of alloyed carbides of type M_6C and of vanadium carbonitrides, which will be referred to as MX particles. The mean massive (> 4 μm) carbide size was less than 5.4 μm for steels T15 and T42 and 6.8 μm for steel T6. The volume fraction of these massive carbides was of 1.1 ± 0.4% for T42, 2.1 ± 0.4% for T15 and 4.5 ± 0.4% for T6 steels. The chemical composition of the primary particles is given in Table IV for the as-sintered specimens and after quenching and tempering. Only one heat treatment condition is reported, because the composition was independent of the austenitizing temperature in the case it was varied (T42) and of the tempering temperature. Noteworthy in Table IV is the existence of two types of particles: one type rich in vanadium, designated as MX, and the other rich in tungsten, molybdenum and iron, designated as M_6C. It is also apparent that the compositions of the different particles are very similar for the different steels and are practically the same in the as-sintered and heat-treated conditions.

TABLE III Details of the heat treatments indicating the austenitizing and tempering temperatures

Steel	Temperature (° C)				
	Aust.	Tempering			
T15	1210	500	525	535	550
		560	575		585
T42	1160	500	550		575
	1190	500	550		585
T6	1275	425	450		480

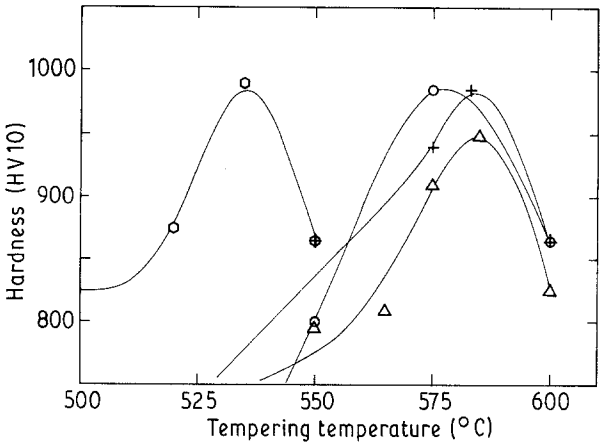

Figure 2 Evolution of hardness with tempering temperature, for triple 1 h tempering, for steels T6 (○), T15 (△). Steel T42 after two austenitizing temperatures (○1160° C, + 1190° C).

Fig. 2 shows the evolution of hardness with the tempering temperature for triple 1 h tempering of the different steels. It is observed that for steel T42 the maximum hardness is reached at a slightly higher temperature (585° C) when austenitized at 1190° C than when austenitized at 1160° C (575° C). In both cases the peak hardness is the same: 985 HV10. Steel T6 reaches the maximum at 535° C with the peak hardness value 990 HV10, being very close to that found in steel T42. Finally the maximum hardness in steel T15, resulting from tempering temperature of 585° C, is 950 HV10, i.e. slightly lower than for steels T42 and T6.

Fig. 3 shows typical microstructures of the three steels for different quenched and tempered conditions. Micrographs 3a and b correspond to steel T15 specimens, triple tempered at 500 and 585° C, respectively, 3c and d to steel T42 tempered at the same

TABLE IV Chemical composition of the different particles as obtained by EDS analysis

Steel	Particle	Condition	W	Mo	V	Cr	Fe	Co
T42	MX	Sintering	9.5	6.5	70.0	6.0	7.0	1.0
		Aust.–Temp. 1190–585° C	7.5	5.5	72.0	6.0	8.0	1.0
	M_6C	Sintering	47.0	20.0	1.5	2.5	25.0	4.0
		Aust.–Temp. 1190–585° C	40.0	21.0	1.0	2.5	24.0	3.5
T15	MX	Sintering	19.0	3.0	61.0	7.0	10.0	0.2
		Aust.–Temp. 1210–575° C	18.6	1.7	61.8	7.1	10.9	0.0
	M_6C	Sintering	62.0	8.0	2.0	2.5	25.0	1.0
		Aust.–Temp. 1210–575° C	61.2	9.2	1.6	2.5	24.7	0.9
T6	MX	Sintering	4.0	1.0	83.7	6.1	4.5	0.9
		Aust.–Temp. 1275–480° C	5.5	0.05	82.7	6.1	4.6	1.0
	M_6C	Sintering	66.4	3.6	1.7	3.1	21.0	4.2
		Aust.–Temp. 1275–480° C	67.9	2.6	1.7	3.0	20.6	4.2

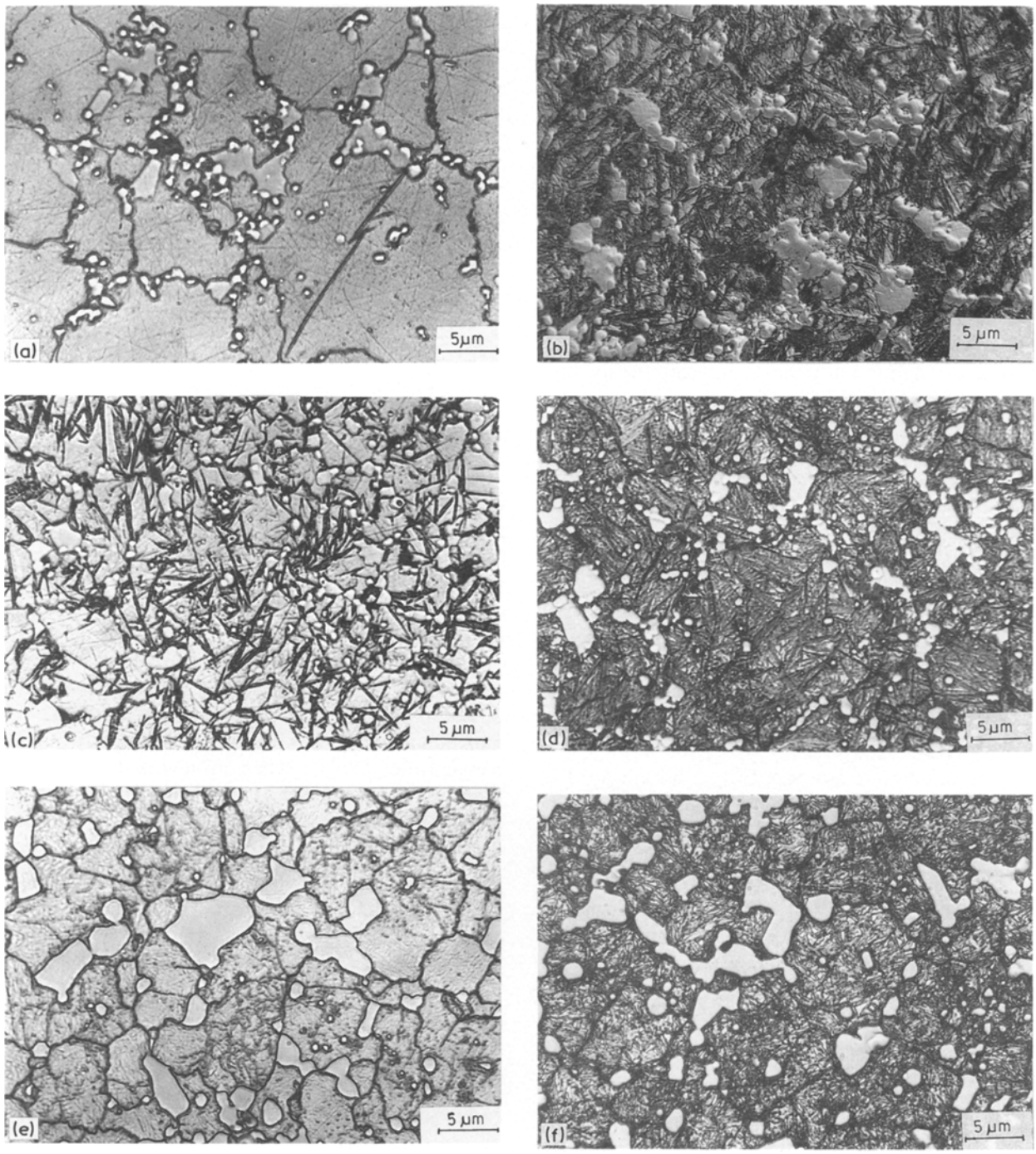

Figure 3 SEM micrographs of quenched and tempered specimens. (a) and (b) T15 at 500° C and 585° C respectively. (c) and (d) T42 at 500° C and 585° C respectively. (e) and (f) T6 at 520° C and 535° C respectively.

temperatures and 3e and f to steel T6 tempered at 520 and 535° C, respectively. It is clearly apparent in micrographs 3a, c and e, which correspond to the lower tempering temperatures and to low hardnesses, that an important amount of retained austenite is present in addition to the primary particles and a small amount of martensite with its classical acicular morphology. It is also apparent for these micrographs that the austenite grain size is bigger in T15 than in the other two steels, as previously pointed out. Whereas in micrographs 3b, d and f, which correspond to the peak hardness for the three steels, no change either in the morphology or the size of primary particles, compared with their corresponding undertempered conditions, is observed, an important increment in the martensite proportion is clearly apparent.

Table V presents the amounts of retained austenite and hardness values found in these steels as a function of processing. Also presented in the Table are the fracture toughness values.

Fig. 4 shows the hardness as a function of the amount of retained austenite; for all the steels, as expected, the hardness increases as the amount of retained austenite decreases. No significant differences of behaviour between the different steels, or in T15 with and without HIPping treatments, are observed. All the experimental data can be fitted to a single line of equation

$$H(HV10) = 960 - 7.0 \times (\%\gamma) \qquad (6)$$

being the 95% confidence limits for the slope of the fitted line in the range 6.2 to 7.7.

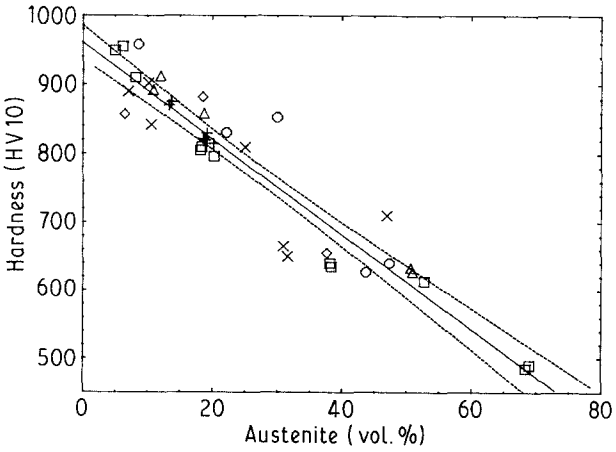

Figure 4 Dependence of hardness on the amount of retained austenite for different quenched and tempered steel. (– – – C. L. 95%). (◇ T15 HIP H2, x T15 HIP HI, + T6 HIP, △ T42 Aust. 1160° C, ⬡ T42 Aust. 1190° C, □ T15 sinter)

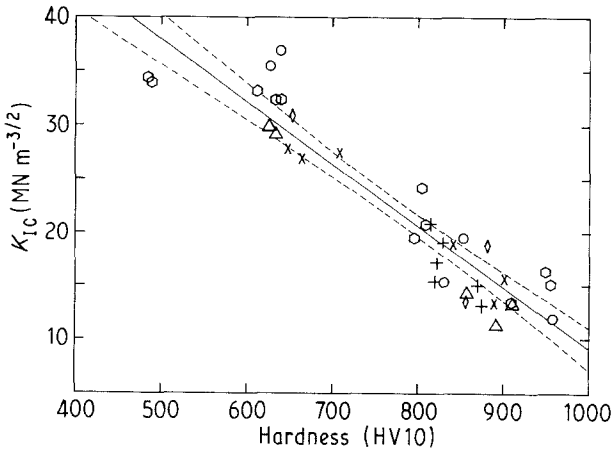

Figure 5 Dependence of fracture toughness on hardness for different quenched and tempered steels (– – – C. L. 95%). (◇ T15 H2, x T15 HI, + T6 HIP, △ T42 Aust. 1160° C, ○ T42 Aust. 1190° C, ⬡ T15 sinter)

Fig. 5 shows the variation of fracture toughness with hardness for the three steels. A clear decrease of toughness with increasing hardness is observed. Within the experimental scatter, all the data can be reasonably fitted to a single straight line, indicating that fracture toughness is related to hardness and is independent of the amount of primary carbides present in the microstructure and of the steel's chemical composition. Again no influence of HIPping is observed. The straight line has the equation

$$K_{Ic}(\mathrm{MN\,m^{-3/2}}) = 66.8 - 0.058 \times \mathrm{H(HV10)} \quad (7)$$

0.058 being the slope within the range 0.05 and 0.065 for the 95% confidence limits.

The fractographic analyses carried out by scanning electron microscopy on the failure surfaces have shown that the fracture modes are very similar in the three steels, being independent of the austenitizing temperature before quenching (T42), or of HIPping (T15). Although all fracture surfaces can be described as quasi-cleavage there were some notable differences – especially observed when stereo pairs were viewed – between the appearance of fracture surfaces of high hardness (low austenite) and low hardness (high retained austenite) steels.

The fractures observed at low hardness (500 HV10) and high retained austenite contents (60 to 70%) are characterized by the presence of large facets, which

TABLE V Summary of mechanical properties of the different high speed steels in terms of the amount of retained austenite produced by several tempering temperatures and processing conditions

Material	State	Tempering temperature (° C)	Retained Austenite	Hardness (HV 10)	K_{IC} (MN m$^{-3/2}$)	r_p (μm)
T15	Sintered	500	69	488	34.3	24.4
		525	53	613	33.3	14.7
		535	38	637	32.5	12.7
		550	20	796	19.7	3.1
		560	18	807	22.2	3.8
		575	18	910	13.6	1.1
		585	5	952	15.9	1.4
T15-H1	Sinter + HIP	525	47	710	27.6	7.5
	1190° C	535	31	658	27.5	8.7
	160 MPa	550	25	810	20.7	3.2
		560	11	842	19.0	2.5
		575	10	902	15.7	1.5
		585	7	890	13.4	1.1
T15-H2	Sinter + HIP	535	38	655	31.0	11.1
	1210° C	560	18	882	19.0	2.3
	140 MPa	585	6	857	13.5	1.2
T42	Sintered	500	51	630	36.9	17.0
	Aust.–1160° C	550	17	858	14.5	1.4
		575	11	902	12.5	1.0
	Sintered	500	45	634	29.8	11.0
	Aust.–1190° C	550	26	842	17.5	2.2
		585	9	975	12.0	0.8
T6	Sinter + HIP	420	20	823	20.1	3.0
	1290° C	450	19	821	16.4	2.0
	140 MPa	485	14	873	14.2	1.3

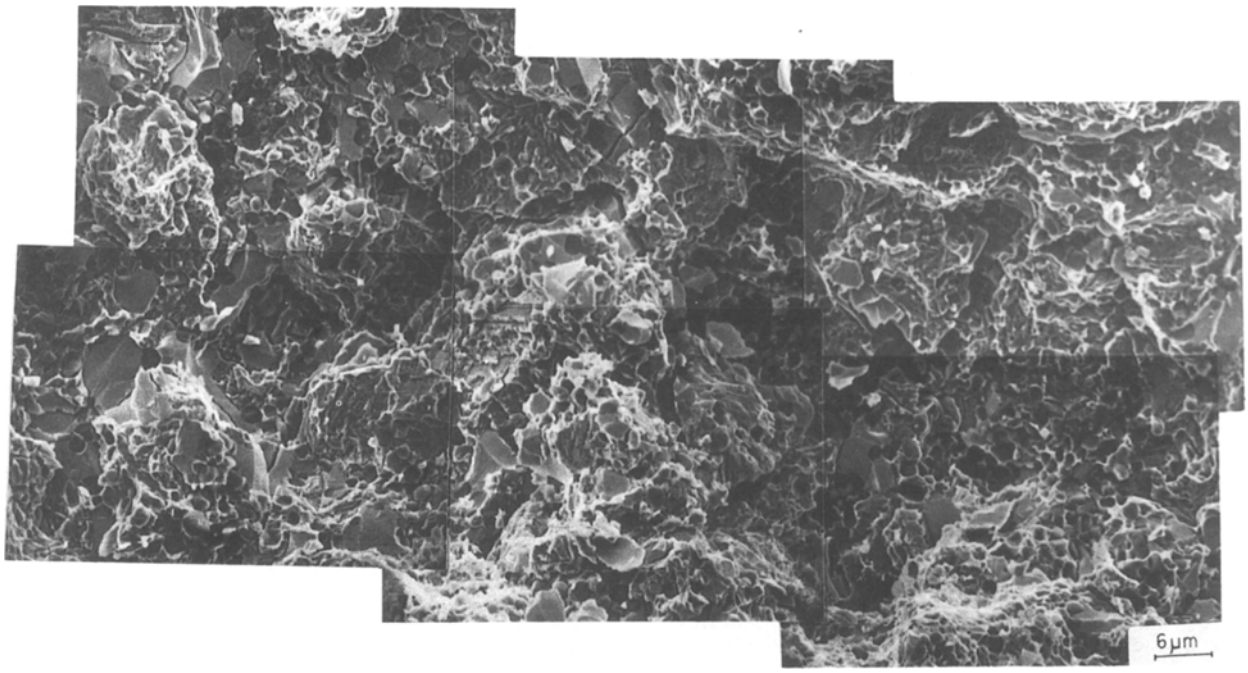

Figure 6 SEM fractograph corresponding to steel T15 tempered at 500° C, giving a low hardness and a high retained austenite content.

seem to correspond to M_6C primary carbides present at the grain boundaries (Fig. 6). The majority of such facets are along (decorating) the grain boundaries. In addition the regions occupied by these carbides seen to form some form of valleys. Indications are, therefore, that cracks run mainly through these primary M_6C carbides at the grain boundaries, with an intergranular character. It is also possible to observe zones of microplasticity associated with microvoids and MX carbonitrides. Some fractured carbides were also observed in the paths of secondary cracks.

For the high hardness steel (950 HV10) and low amounts of retained austenite (less than 10%), the fracture surface can be differentiated from the previous by a flat aspect, showing no evidence of the "valleys". It can be observed that the size of the facets has decreased, but their amount has increased (Fig. 7). In this case the grain boundaries, decorated with M_6C, do not seem to be the preferred path for the advancing crack its propagation being controlled by the matrix, not the carbides. In this case microplasticity is also not as prevalent.

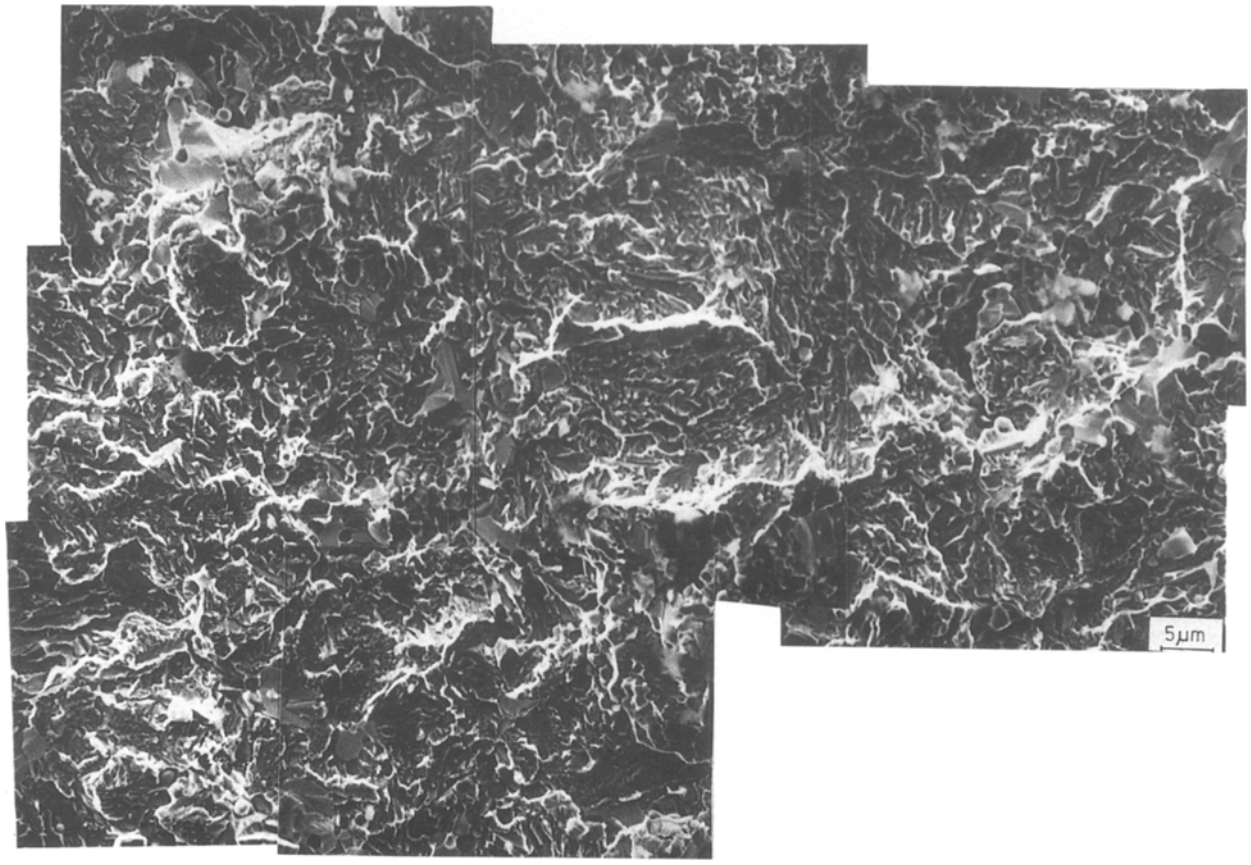

Figure 7 SEM fractograph corresponding to steel T15 tempered at 585° C, giving a high hardness and a low retained austenite content.

4. Discussion

The mean and maximum carbide sizes obtained in steels T42, T15 and T6 (Fig. 3) are close to those found in dense products processed both by vacuum sintering [18–20] and gas sintering in the same atmosphere [20, 21]. M_6C carbides are rich in tungsten, molybdenum and iron, but also contain small amounts of cobalt. Similar compositions are reported by several authors [22–24]. The present results are also in agreement with what was found earlier, i.e. that the higher the cobalt content of the steel, the bigger its content in the carbide [25].

The peaks in hardness are reached in the present steels at higher temperatures than previously reported for steels with similar nominal composition. This would be relevant in continuous cutting with considerable heat generation. For instance, the maxima in hardness in steels T15 and T42 are reached after triple tempering at 585° C, this is about 60° C above the 525° C, reported by Wright *et al.* [26] for steel T42 sintered under vacuum and about 45° C above the 540° C reported by Beiss *et al.* [23] for similarly processed T15. On the other hand, the temperature for the peak found for steel T6 of 535° C is 15° C above the 520° C reported both for a sintered steel and a conventional wrought product [10]. The reason for the need of higher tempering temperatures to reach peak hardness in these steels is the high amount of nitrogen picked-up during their sintering in the N_2–H_2–CH_4 atmosphere used. As pointed out in a previous paper [20] considerable amounts (0.3 to 0.6% nitrogen) can be picked-up during the sintering operation. This has several consequences, including the change of MC type carbides to MX carbonitrides and the appreciable increase in the amount of retained austenite after quenching, as shown in Table V. It seems that for its elimination i.e., to transform it to martensite, which is fundamental in reaching the maximum hardness, the higher temperatures are necessary. Work is currently in progress [27] to investigate the details of the retained austenite transformation after multiple temperings.

Fracture toughness determination was by the, relatively unestablished, Barker [14], short rod method which does not involve sharp precracking, usually performed by fatigue [28] or impact wedge [29] techniques, more commonly employed for high speed steels.

Fig. 8 is a micrograph of a section cut perpendicularly to the fracture surface in a failed short rod specimen of steel T42, quenched from 1190° C and triple tempered at 585° C. The presence of some isolated pores close to the fracture surface is clearly apparent. They seem to be connected by secondary fracture branches perpendicular to the failure surface. This clearly means that in this kind of test the fracture is completely determined by the path defined by the cut (notch) made in the specimen.

It is worth emphasizing that the present results on T42 and those reported by Wright *et al.* [26] on a similar material, but obtained using pre-cracked specimens, are very close for the same hardness values. Fig. 9 plots all K_{IC} data measured in the present work, together with previously published on T6 and T42, but

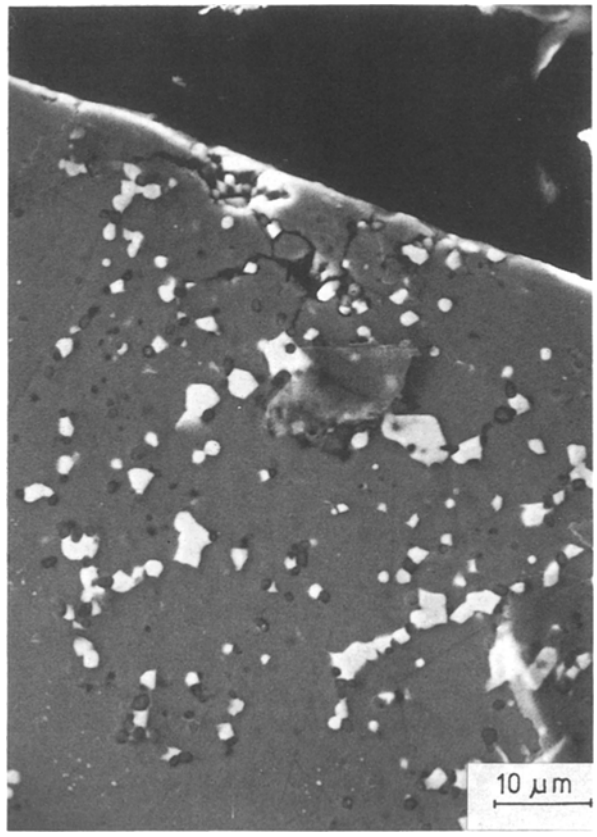

Figure 8 SEM micrograph of a perpendicular cut to the fracture surface in steel T42 quenched from 1190° C and tempered at 585° C.

but also M2, M7 and M42. The present results – with their 95% confidence limits – cover the entire range of HV and K_{IC} and should be seen as an important contribution to the data base on which comprehensive microstructural models are to be based.

The toughness in high speed steels has been inversely correlated with hardness [6, 30], and interpreted as mainly related to the matrix properties and not to the amount, size and morphology of the primary carbides. Bearing in mind the correlation between fracture toughness and hardness (Fig. 5) and that between hardness and the amount of retained austenite

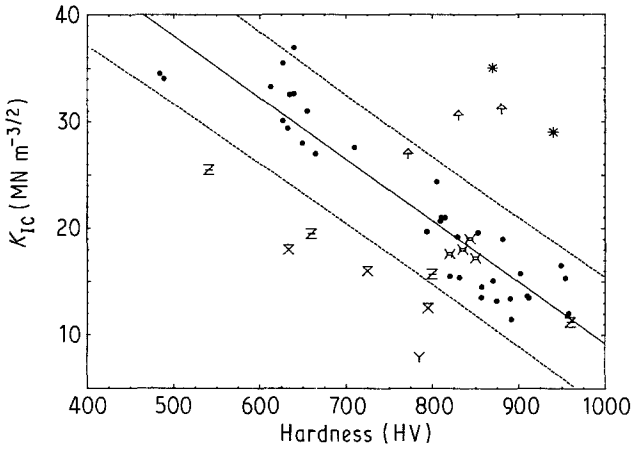

Figure 9 Comparison of the present work results on fracture toughness with other results found in the literature. Broken lines represent the 95% confidence limits of the present work results. (* T6 [11], ×T42 [26l], ϒ M42 [5], ⧗ MT [5], ⧖ M2 [6], ⧗ M2 [31], ● T15 PW HIP H2, T15 PW HIP H1, T6 PW HIP, T42 PW aust. 1160° C, T42 PW aust. 1190° C, T15 PW)

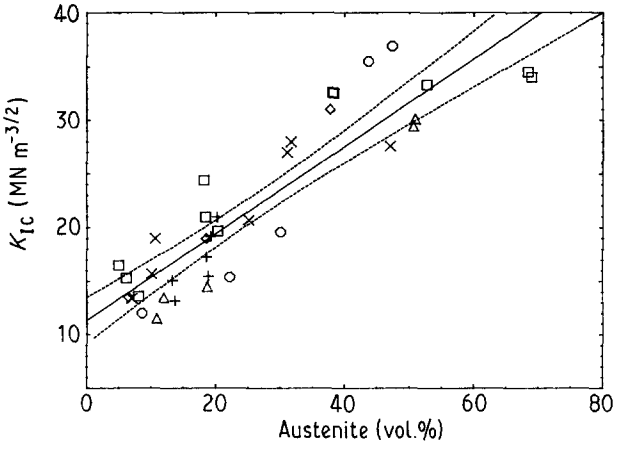

Figure 10 Dependence of fracture toughness on the amount of retained austenite for all the materials and treatments used in the present work. Broken lines are 95% confidence limits. (◇ T15 HIP H2, x T15 HIP H1, + T6 HIP, △ T42 aust. 1160° C, ⬡ T42 aust. 1190° C, □ T15 sinter)

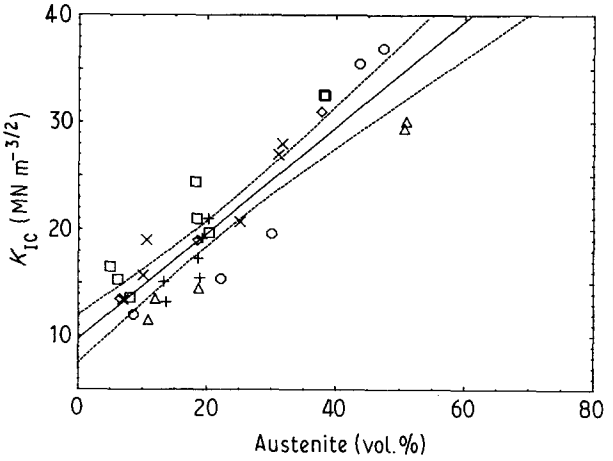

Figure 11 As in Fig. 10, without considering the data points in the region of saturation of fracture toughness dependence on retained austenite.

(Fig. 4), it is reasonable to postulate a dependence of fracture toughness on the amount of retained austenite. This relationship is shown in Fig. 10, in which fracture toughness, measured by the short rod method, is shown plotted against the amount of retained austenite for the three steels with the different heat treatments. It is clearly apparent that increasing the amount of retained austenite results in an increase in fracture toughness. Additionally, it can also be observed that variables as composition (T15, T42 or T6), thermomechanical treatments, as HIP, do not have a large influence on fracture toughness. All the experimental data can be fitted to a straight line of equation

$$K_{Ic}(\mathrm{MN\,m^{-3/2}}) = 11.3 + 0.41 \times (\%\gamma) \quad (8)$$

The 95% confidence limits for the slope of the adjusted straight line are within 0.34 and 0.48.

It is also considered instructive to evaluate the plastic zone, r_p, sizes; these are presented in Table V. It is seen that, with few exceptions, the sizes of these zones are smaller than the (prior austenite) grain sizes and thus the crack can be thought to be under the influence of several microstructural features. In particular for the low austenite (high H_v) materials r_p is comparable to the size of the carbides, whereas at low HV, is of the order of the austenite grain size. The absolute values of r_p, 1 to 24 μm, cover the range reported for T42 (0.3 to 3.0 μm), M2 (up to 30 μm) and T1 and T6 (2 to 6 μm) and therefore, as with K_{Ic}, indicate the possibility of, through control of the amount of retained austenite, control of microstructurally dependent macroscopic engineering properties.

When Fig. 10 is closely examined, it is evident that, for T15 H1 above 35% retained austenite and for just sintered T15, above 40% retained austenite there is no detectable affect on K_{Ic}. If these results are neglected (Fig. 11) relation (8) becomes

$$K_{Ic}(\mathrm{MN\,m^{-3/2}}) = 9.9 + 0.50 \times (\%\gamma) \quad (9)$$

but the 95% confidence limits are virtually unaltered, being between 0.42 and 0.58.

It seems therefore that, whereas the hardness retained austenite (Fig. 4) relationship does not have a cut-off point, one, near 50% retained austenite, appears to exist for toughness. This should be promising in the context of microstructurally optimizing combination of toughness and wear resistance, as the latter appears more dependent on type, distribution and size of carbides than microscopic hardness.

5. Conclusions

The conclusions are as follows.

(1) The sintering of T6, T15, T42 specimens in the N_2–H_2–CH_4 atmosphere has a large nitrogenation effect, which is reflected in the change of MC carbides to fine carbonitrides, and also stabilizes the austenite; being tempering at higher temperatures necessary to eliminate it.

(2) The short rod method to measure fracture toughness in these materials seems to be validated when comparison of values for similar materials measured using conventional precracked specimens is made.

(3) A good correlation between hardness and retained austenite is observed in all three materials.

(4) A good correlation, as also found by other workers, exists between fracture toughness and hardness. In this case the correlation has been extended to a very broad range of hardness values associated with different microstructures.

(5) A good correlation between fracture toughness and the amount of retained austenite has not been established. It seems that the effect of improving fracture toughness of high speed steels by austenite is less effective for high austenite amounts.

(6) The fractographic analyses show that, although fracture modes can be described as "quasi-cleavage", some local plasticity can be observed, particularly in materials with low hardness and high retained austenite content.

(7) The present results clearly show that a very broad range of controlled microstructures, hardnesses and values of fracture toughness can be obtained in these group of high speed steels after sintering in the N_2–H_2–CH_4 atmosphere.

Acknowledgements

The authors wish to thank Dr Wronski of the Uni-

versity of Bradford for stimulating discussions during the writing of this paper and thank the CICYT for financial support. V. Martínez and R. H. Palma thank the Universidad de Santiago and the Universidad de Atacama (Chile) respectively for the leave of absence.

References

1. B. L. AVERBACH, B. LOU, P. K. PEARSON, R. E. FAIRCHILD and E. N. BAMBURGER, *Metall. Trans.*, **16A** (1985) 1253–1271.
2. B. L. AVERBACH, *Met. Prog.* **118** (1980) 19–24.
3. J. A. RESCALVO and B. L. AVERBACH, *Metall. Trans.*, **10A** (1979) 1265–1271.
4. A. R. JOHNSON, *ibid.* **8A** (1977) 891–897.
5. K. ERICKSSON, *J. Scand. Metall.* **2** (1973) 197–203.
6. S. C. LEE and F. J. WORZALA, *Metall. Trans.* **12A** (1981) 1477–1484.
7. L. R. OLSSON and H. F. FISCHMEISTER, *Powder Metall.* **1** (1978) 13–28.
8. D. A. CURRY and F. J. KNOTT, *Met. Sci.* **13** (1979) 341–345.
9. H. F. FISCHMEISTER, "Special Steels and Hard Materials", 1988, (Pergamon Press, Oxford, 1988) pp. 127–140.
10. A. S. WRONSKI, L. B. HUSSAIN AL-YASIRI and F. L. JAGGER, *Powder Metall.* **22** (1979) 109–118.
11. P. W. SHELTON and A. S. WRONSKI, *Mater. Sci. Technol.*, **3** (1987) 260–267.
12. R. H. PALMA, V. MARTINEZ and J. J. URCOLA, *Revista de Metalurgia CENIM*, (1989) in press.
13. V. MARTINEZ, Master Thesis, ESII, University de Navarra, Spain (1987).
14. L. M. BARKER: Terratek Report, TR81-07, (1981).
15. J. R. TINGLE, C. A. SHUMAKER, Jr., D. P. JONES and R. A. CUTLER, "Chevron-Notched Specimens: Testing and Stress Analysis", (ASTM, Philadelphia, 1984) pp. 281–296.
16. L. M. BARKER and F. I. BARATTA, *J. Testing and Evaluation*, **8** (1980) 97–102.
17. R. L. MILLER, *Trans. ASM*, **57** (1964) 892.
18. R. H. PALMA, V. MARTINEZ and J. J. URCOLA, in Proceedings II Congress Mundial Vasco, 1987, Bilbao, España.
19. W. J. C. PRICE, M. M. REBBECK, A. S. WRONSKI and S. A. AMEN, *Powder Metall.* **28** (1985) 1–6.
20. R. H. PALMA, V. MARTINEZ and J. J. URCOLA, *Powder Metall.* **32** (1989) 291–299.
21. J. V. BEE, J. V. WOOD, P. R. BROWIN and P. D. NURTHEN, in Proceedings Powder Metallurgy Meeting, Sept. 1985, San Francisco, USA.
22. A. FISHER and E. AOLLHAS, *Pract. Metall.* **12** (1975) 393–406.
23. P. BEISS and M. T. PODOB, *Powder Metall.* **25** (1982) 69–74.
24. K. STILLER, L. E. SVENSSON, P. R. HOWELL, W. RONG, H. O. ANDREW and G. L. DUNLOP, *Acta Metall.* **32** (1984) 1457–1467.
25. G. A. ROBERTS and R. A. CARY, in "Tool Steels", 4th edn (ASM, Metals Park, Ohio, 1980).
26. C. S. WRIGHT, A. S. WRONSKI and M. M. REBBECK, *Met. Technol.* **11** (1984) 181–188.
27. I. URRUTIBEASCOA, R. H. PALMA and V. MARTINEZ, Current work at CEIT.
28. British Standard, BS 5447: 1977, 1–11.
29. K. ERIKSSONN, *Scand. J. Metall.* **4** (1975) 182–184.
30. O. E. OKORAFOR, *Mater. Sci. Technol.* **3** (1987) 118–124.
31. P. W. SHELTON and A. S. WRONSKI, *Met. Sci.* **17** (1983) 533–539.

Received 6 April
and accepted 14 September 1989